e-ISSN 2320 –7876 www.ijfans.org
Vol.11, Iss.11, 2022

CONSTITUTIVE MODEL FOR DENSIFICATION OF SINTERED PREFORMS OF AL-TiB_2 DURING HOT UPSETTING

[1]Md Ahasan, [2]Dr .Ch. Shashikanth

[1]Professor & H.O.D, Dept. of Mechanical Engineering, DNR College Of Engineering And Technology, Bhimavaram, A.P, India.

[2]Associate professor, Dept. of Mechanical Engineering, Sree Chaitanya College of Engineering, Karimnagar, A.P, India.

Abstract

The main aim of this paper is to evaluate the effect of the relative density on hot deformation behaviour, model and predict the flow stress of the sintered compacts using constitutive equations. Hot compression behaviour of Aluminium-Titanium Diboride alloy sintered compacts was studied by performing hot deformation test in 50 ton hydraulic machine. For this purpose, Al-5%TiB2 composition has been sintered with different relative densities of 0.80, 0.85 and 0.90 which have been prepared by cold pressing. The compacts were hot compressed at different temperatures of 200^{o}C, 300^{o}C, 400^{o}C and 500^{o}C at different strain rates of 0.12s^{-1}, 0.14s^{-1}, 0.16s^{-1} and 0.18s^{-1}. The graphs are plotted for deformation temperature and strain rate. Flow stress of the powder compacts was described by Zener-Hollomon parameter in an exponential equation containing relative density, compensated material constants and also the deformation energy of activation. As the deformation temperatures and the strain rate were increased and the density decreased, a decrease within the flow stress level was observed.

1. Introduction

Aluminium metallurgy , reduces or eliminates the capital and operational prices related to machining operation to get close to internet formed components by combining versatile properties of Al with the flexibility of PM [1-2]. Aluminium metallurgy plays a superior role in analysing the extreme temperature physical property of Al -2014, during a big selection of temperatures and strain rates. Bardi et al [3] analysed the dependence on stress and temperature by means of conventional constitutive equations and by a modified sinh-equation where stress was substituted by an efficient stress i.e. the difference between actual stress and threshold stress. Shao et al. [4] used hot compression tests for investingating the hot workability and constituent flow behaviour of powder metallurgy processed 20 vol.%SiCp/2024Al composite. They presented the modified Arrhenius-type constituent equations with the values of material constants as a function of strain. Narayanasamy et al.[5]. evaluated hot forging features in pure iron mould preforms and by experimentation analysed the connection of theoretical density with new geometrical shape factor and studied the influence of densification on various parameters like geometrical form, stress magnitude relation parameter and barrel radius happens throughout the plastic deformation. In hot deformation method, specifically the extrusion and forging sound data on the new deformation of a cloth is most vital [6-8].The main important processing parameters like deformation temperature, strain rate and material properties, such as microstructure and chemical composition of the material, these parameters are affecting the hot deformation flow stress. Therefore, several studies have been performed to analyse the effect of working parameters on the hot deformation behaviour of aluminium and its alloys [9-13]. Additionally hot deformation flow stresses may be predicted, by modelling the flow stress behaviour of various aluminium materials and proposed constitutive equations are consider effect of the deformation temperature and the strain rate [14-16]. The work carried out on the hot deformation behaviour of porous aluminium alloy are relatively scarce. Meagre due to lack knowledge in the respective field because of the dearth of information within the field, the studies on the new deformation behaviour are relatively rare [17-20], and evaluated the consequences of the relative green density deformation and strain rate on the deformation behaviour and flow stress of powder compacts cold pressed from an commercial Al-Zn-Mg-Cu premix [21-22]. The important theme of the many studies is that the hot deformation behaviour of bulk aluminium alloys [23-25].

The present study deals with the constitutive equation of sintered Al-5%TiB2 during hot deformation, at different temperatures (200^{o}C 300^{o}C 400^{o}C 500^{o}C), strain rates (0.12 0.14 0.16 0.18) and densities (80%, 85%, 90%) and located the values of Q, A, β, α by plotting various graphs.

2.1 **Experimental work**

Aluminium (Al) powder of particle size - 46 µm was obtained from SRL laboratories mumbai, India. titanium Diboride (TiB2) powder was obtained from Alfa Aesar, A Johnson Mathey Company, Hyderabad, India. Desired amount of the powders of Al and TiB2 were weighed and alloyed employing a ceramic ware bowl by stirring manually. The alloyed Al-5%TiB2 and Al-10%TiB2 composites were poured into a die of size 15 mm diameter and thirty mm height and therefore the walls of the die was lubricated with zinc stearate powder . The preforms were prepared with completely different relative densities particularly 0.80, 0.85 and 0.90 on a mechanical hydraulic press of 0.5MN capacity. The compacts were sinterd at a temperature of 550^{o}C for one hour in a tubular furnace under argon gas atmosphere. The preforms were heated in a furnace to the desired temperatures and maintained for 1 hr at the required temperature for homogeneous distribution of temperatures. The preforms were hot compressed at different temperatures particularly 200^{o}C, 300^{o}C, 400^{o}C, 500^{o}C and at different strain rates particularly 0.12, 0.14 0.16 and 0.18. The required compressive load is given to the sample by the ram of the machine once the sample still within the chamber. the top contact diameter (Dtop), the bottom contact diameter (D bottom), the bulge diameter (Db) and therefore the final height (Hf) were noted by using digital vernier calliper and therefore the density was measured by Archimedes' principle. of the distorted compacts before and once each step of deformation. From the measured dimensions, the conventional stress (σz), normal strain (εz). and constitutive parameter values were found.

e-ISSN 2320 –7876 www.ijfans.org
Vol.11, Iss.11, 2022
 UGC CARE Listed (Group -I) Journal

2.2 **Constitutive analysis**

In hot compression of metallic material, the relationship between the flow stress of the material and deformation parameters, such as the deformation temperature and strain rate can be expressed as [26]

$$z = \dot{\varepsilon}\, exp\left(\frac{Q}{RT}\right) = F(\sigma) \text{------} \quad (1)$$

$$\dot{\varepsilon} = Z\, exp\left(-\frac{Q}{RT}\right) = F(\sigma)\exp\left(-\frac{Q}{RT}\right) \text{------} \quad (2)$$

Where Z (Zener-Hollomon parameter) is the deformation corrected strain rate, $\dot{\varepsilon}$ is the strain rate (s^{-1}), Q is the activation energy of hot deformation (J/mol), R is the gas constant (8.31 $Jol^{-1}\ K^{-1}$), and T is the absolute temperature (K). F(σ) is called the stress function and corresponds to one of the following equation depending on the deformation conditions:

$$F(\sigma) = A_1\sigma^m = Z \text{------} (3)$$

$$F(\sigma) = A_2 \exp(\beta\sigma) = Z \text{------} (4)$$

$$F(\sigma) = A_3 [\sinh(\alpha\sigma)]^n = Z \text{------} (5)$$

3. Results and Discussions:

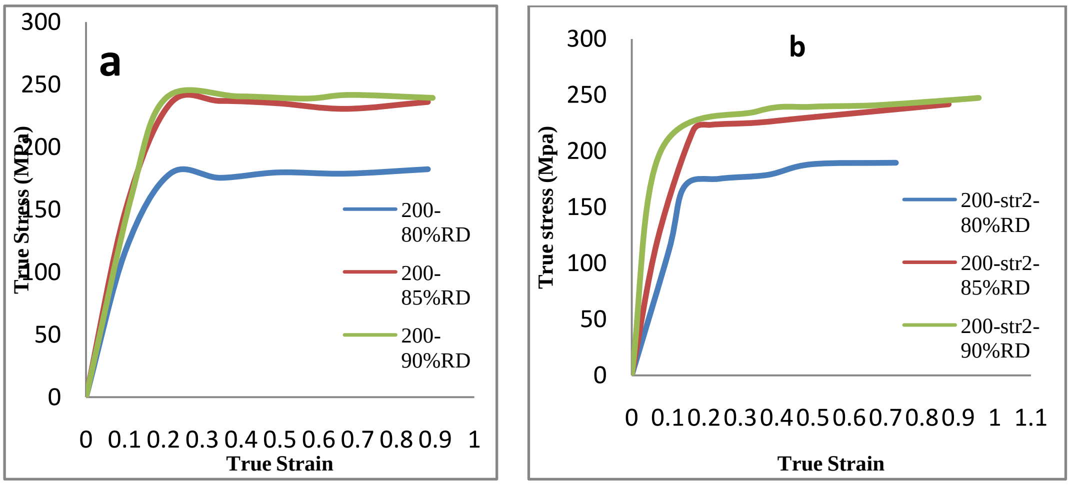

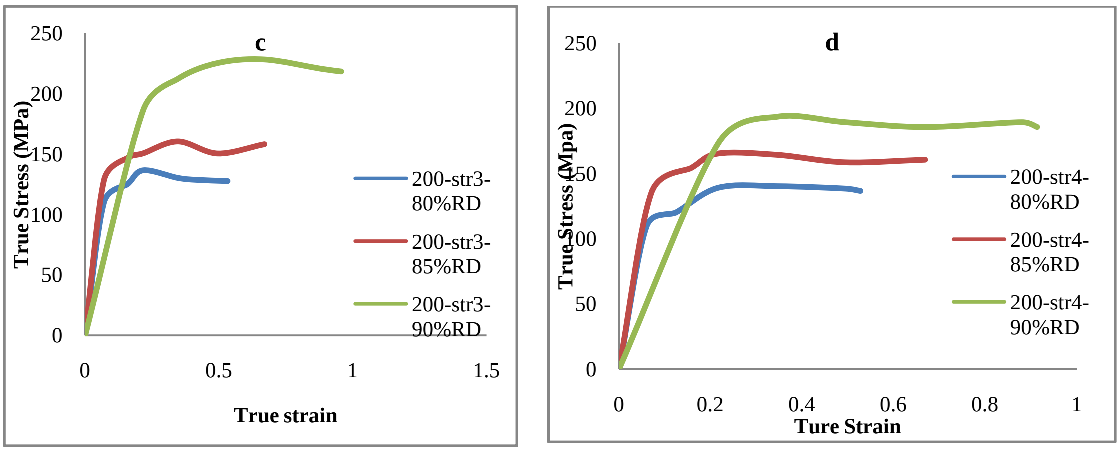

Fig.1. True stress-true strain curves of sintered Al-5%TiB2 powder compacts hot compressed at 200^{o} C and different strain rates (a) 0.12 s^{-1} (b) 0.14s^{-1} (c) 0.16s^{-1} (d)0.18s^{-1}.

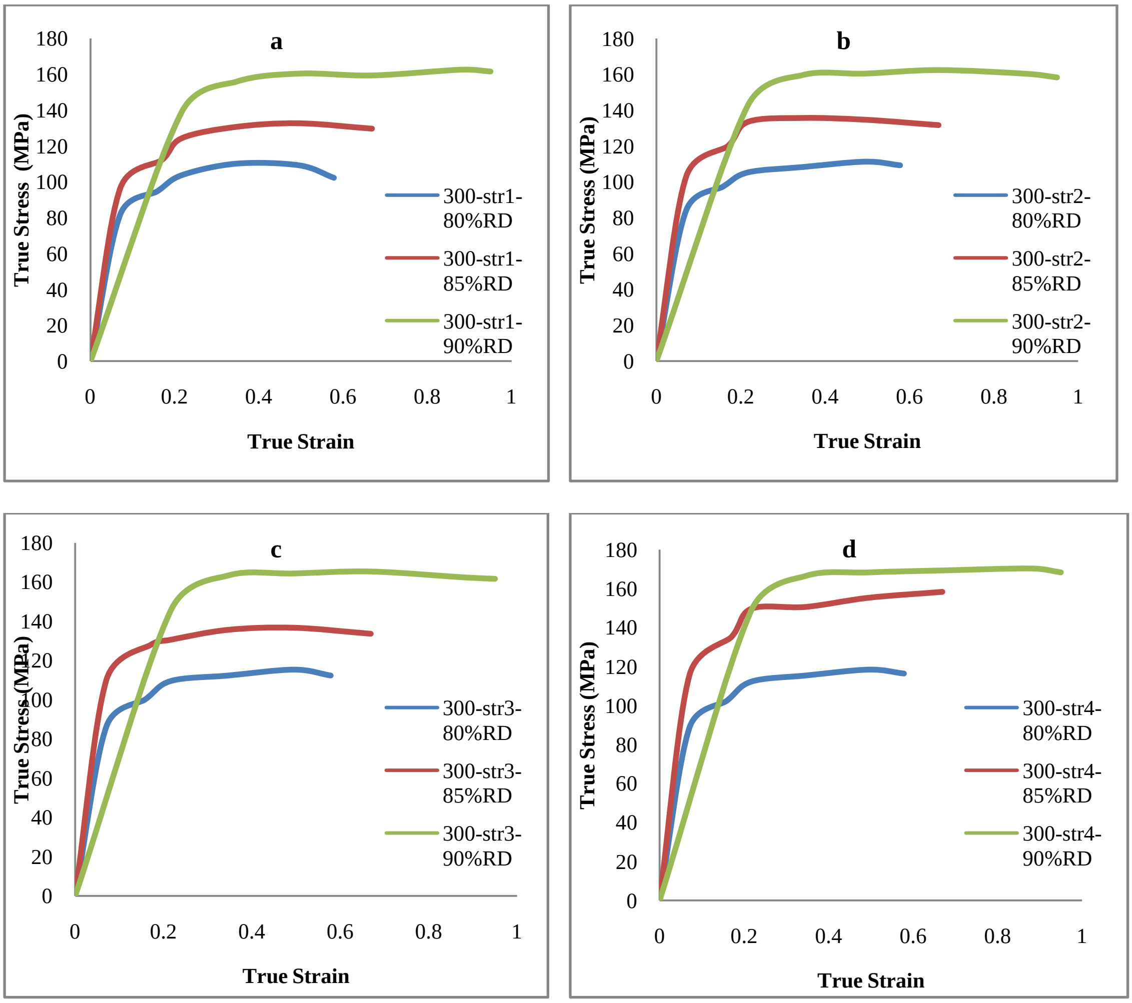

Fig.2. True stress-true strain curves of sintered Al-5%TiB2 powder compacts hot compressed at 300^{o} C and different strain rates (a) 0.12 s^{-1} (b) 0.14s^{-1} (c) 0.16s^{-1} (d)0.18s^{-1}.

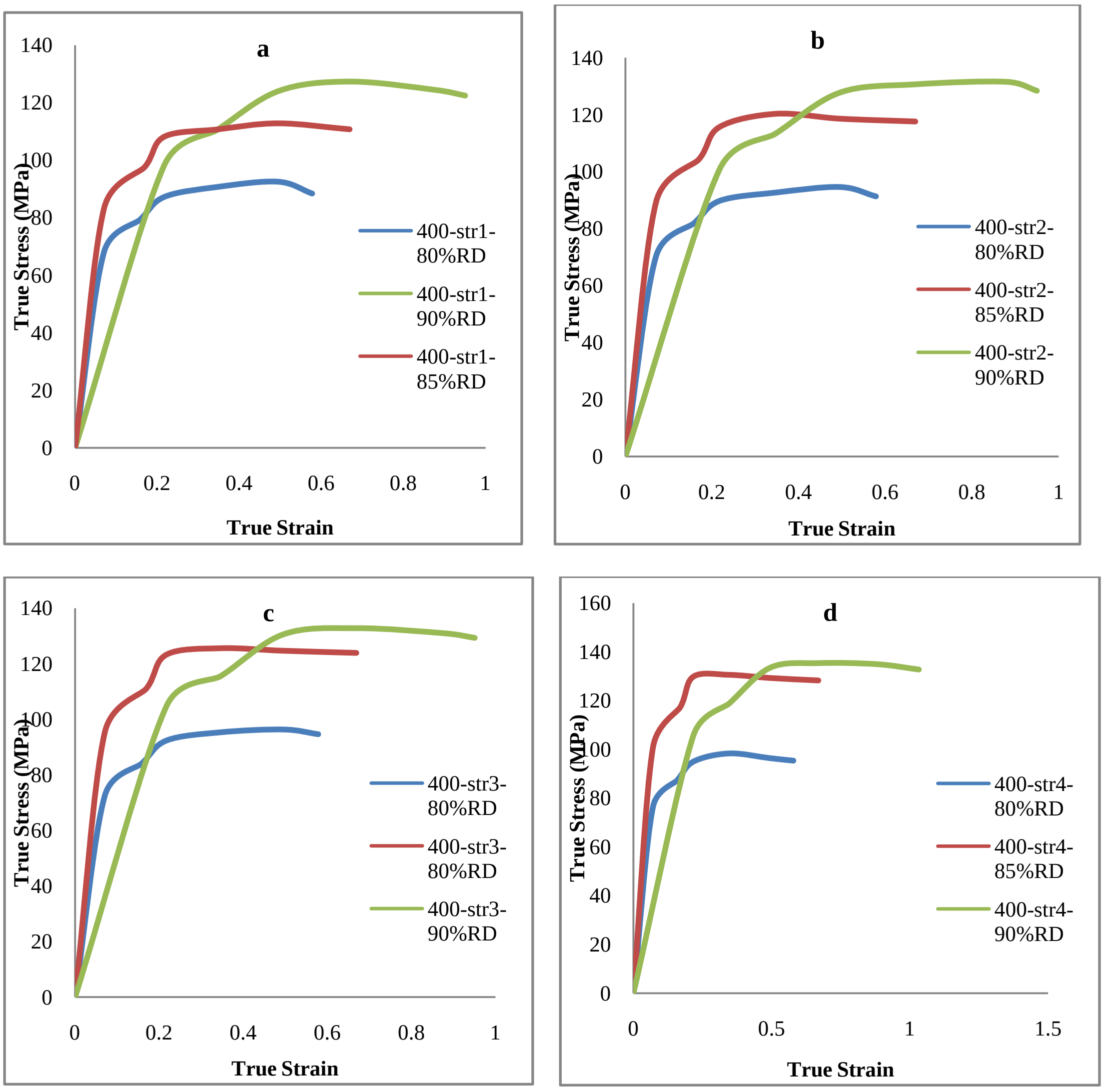

Fig.3. True stress-true strain curves of sintered Al-5%TiB2 powder compacts hot compressed at 400^{o} C and different strain rates (a) 0.12 s^{-1} (b) 0.14s^{-1} (c) 0.16s^{-1} (d)0.18s^{-1}.

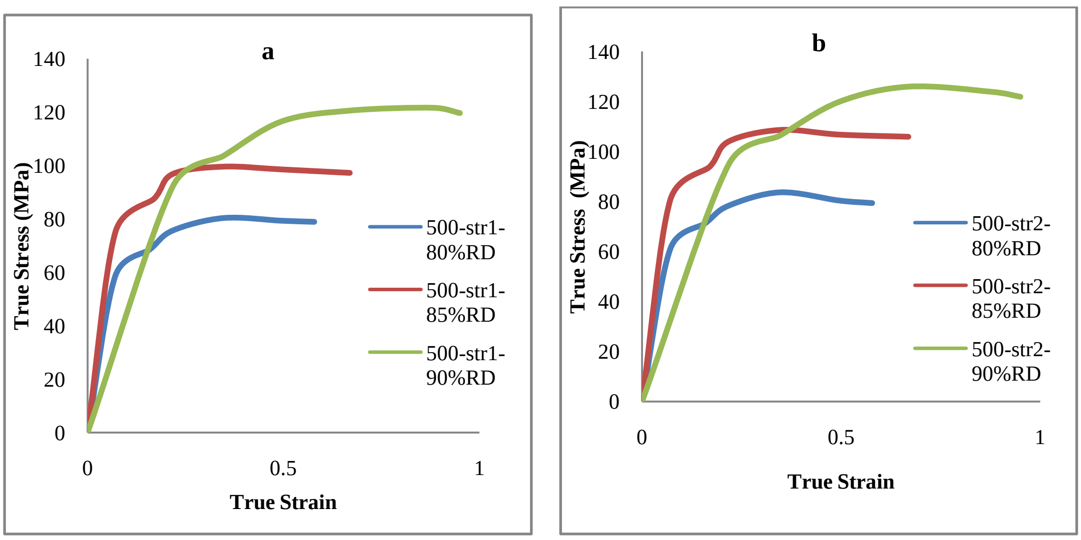

e-ISSN 2320 –7876 www.ijfans.org
Vol.11, Iss.11, 2022
  UGC CARE Listed (Group -I) Journal

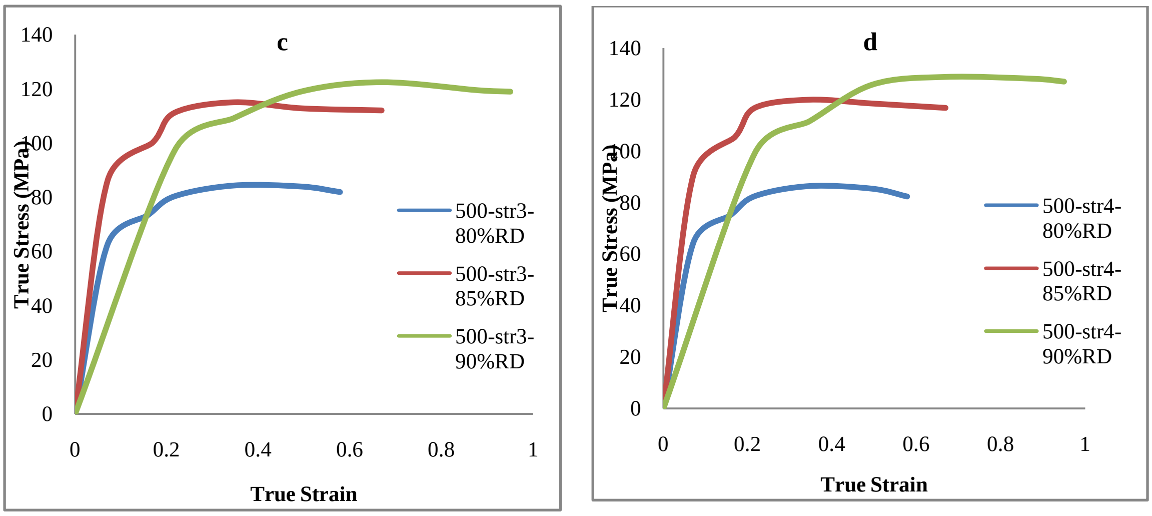

Fig.4. True stress-true strain curves of sintered Al-5%TiB2 powder compacts hot compressed at 500^{o} C and different strain rates (a) 0.12 s^{-1} (b) 0.14s^{-1} (c) 0.16s^{-1} (d) 0.18s^{-1}.

The fig.1 to 4 shows the characteristics of stress- strain curves during hot compression process, it is noticed that the influence of strain rate and temperature on flow stress is significant. The flow curve indicates strain hardening initially, after peak stress it follows steady state at low strain rates and softening at high strain rates. It is observed as the deformation temperature increased or strain rate and relative density decreased a decrease in peak stress. For porous material during the deformation process at high temperature hardening mechanisms such as densification, and softening mechanisms such as recrystallisation and dynamic recovery can occurs simultaneously. At the starting of deformation, dislocation density increases rapidly which leads to quick increase in peak flow stress.

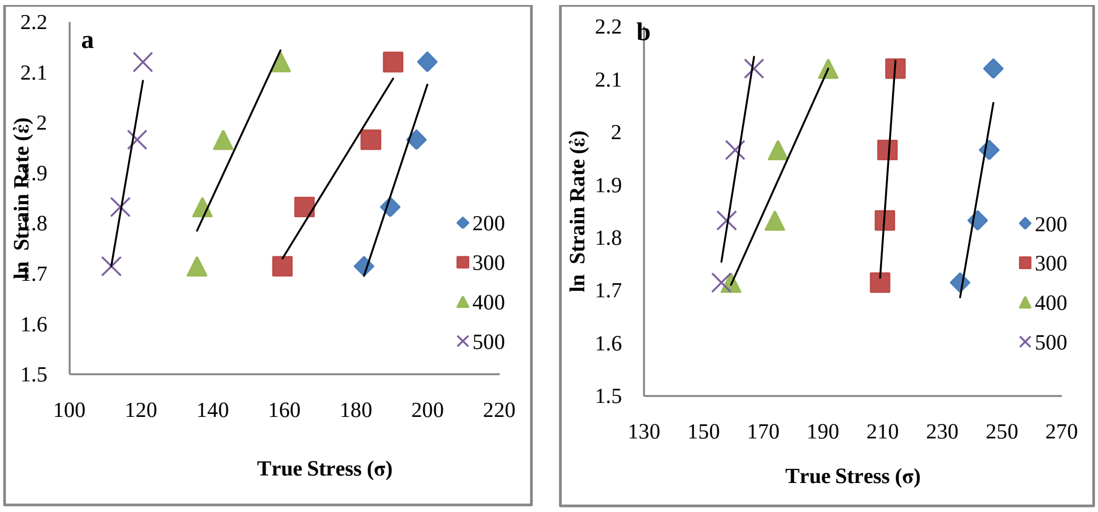

e-ISSN 2320 –7876 www.ijfans.org
Vol.11, Iss.11, 2022
  UGC CARE Listed (Group -I) Journal

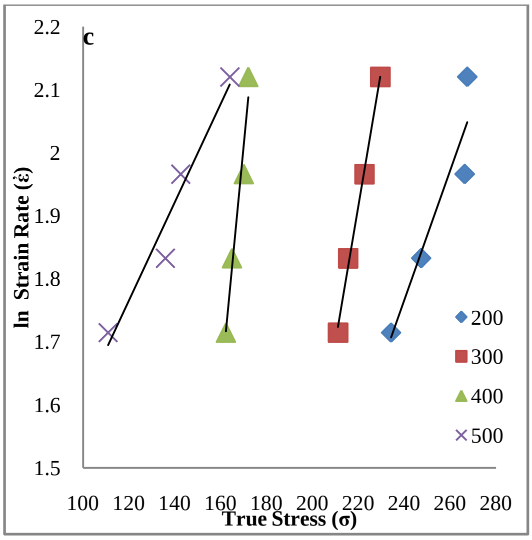

Fig.5 Relationship between the peak flow stress (true stress) for powder compacts with different relative densities (RGD): RGD-80% (a), RGD-85% (b), RGD-90% (c).

From Fig.5 shows the value of ln $\dot{\varepsilon}$ as a function of stress at constant temperature for different powder compacts with different relative densities. The average slope of the line obtained at a temperature for each powder compacts was considered to an evaluation of the βfor each compacts. Consequently, these values were used to estimate the deformation activation energy (Q) of each powder compact.

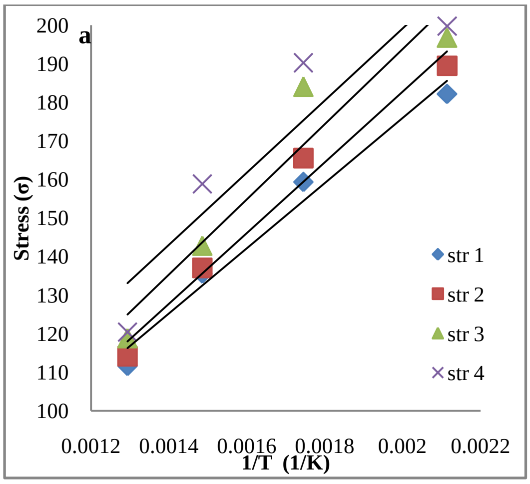

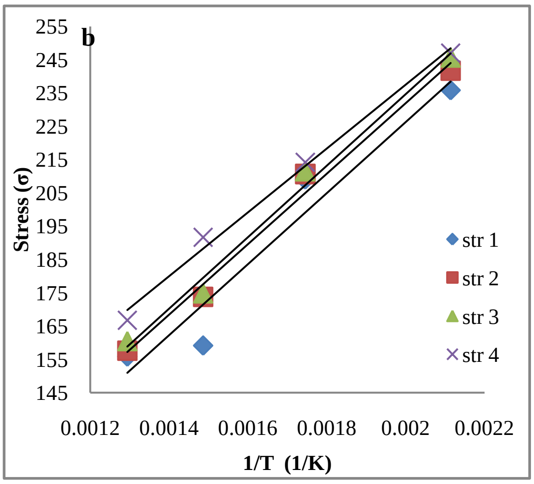

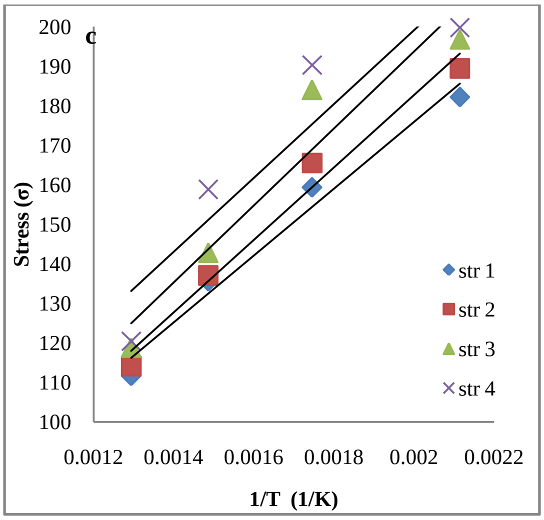

Fig.6. Relationship between the peak flow stress (true stress) and (1/T) for powder compacts with different relative densities (RD): RD=80% (a) RD=85% (b) RD=90% (c).

The value of true stress as a function of (1/T) at constant strain rate for different powder compacts with different relative densities is shown in Fig.2. The average slope of the lines attained at a constant strain rate for each powder compact was used to calculate the value of Q for each powder compact.

The relative density of the powder compacts has significant effect on the value of Q and β. As Q increased with increase of the relative density, Q the deformation activation energy is indicator of the difficulty of deformation. Table 1 presents values of β and Q for each powder compact, which were found from Fig.1 and 2. As shown in the table 1 the value of Q decreases with decrease of relative density. Porous material reduces the resistance to deformation due to the porous present in the structure.

Table 1 .The value of β and Q for the powder compacts with different relative densities.

Relative density (%)	β	Q (j/mol)
80.0	0.02865	28708.19
85.0	0.02405	35543.53
90.0	0.02285	38552.33

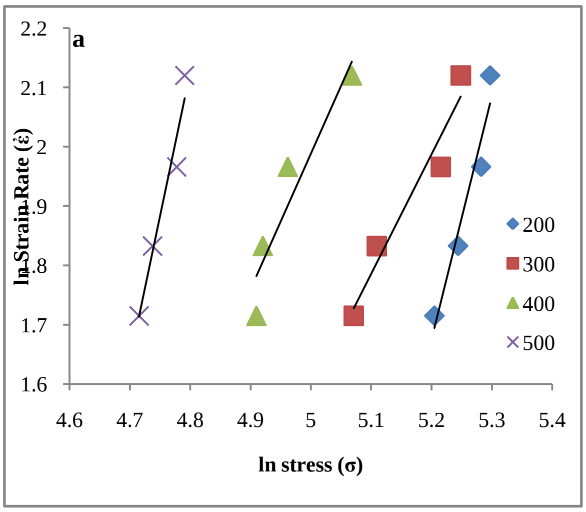

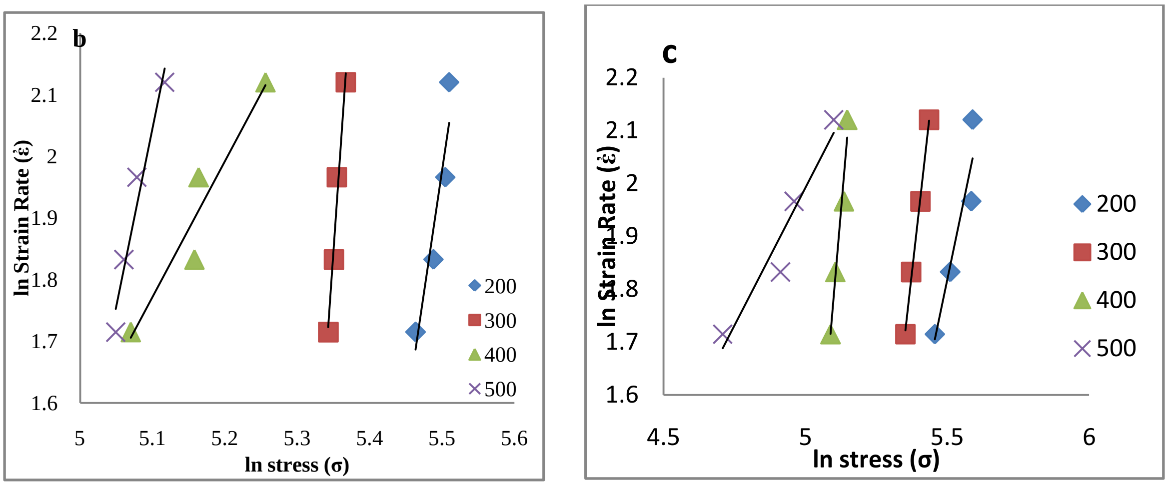

Fig.7. Relationship between ln strain rate (ε̇) and ln stress for powder compacts with different relative densities (RD): RD=80% (a) RD=85% (b) RD=90% (c).

Fig.3. shows the value of ln $\dot{\varepsilon}$ and ln σ (true stress) at constant temperature for different powder compacts with different relative density. The average slope of the lines obtained at constant temperature for each compact was considered to be calculating the value of n for each compact. Subsequently these values were used to found the β value for each powder compact.

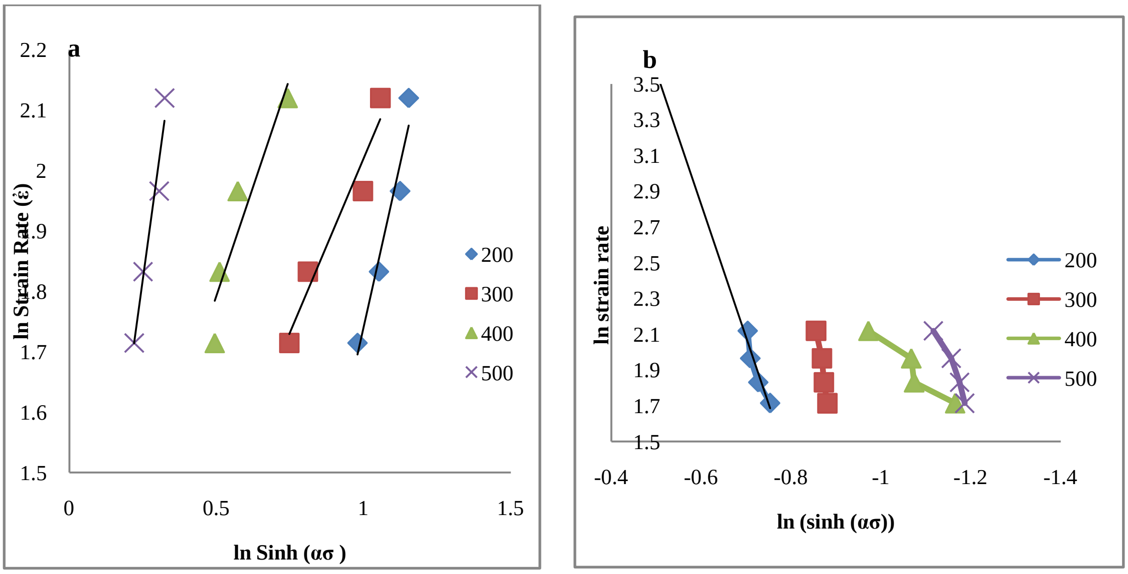

e-ISSN 2320 –7876 www.ijfans.org
Vol.11, Iss.11, 2022

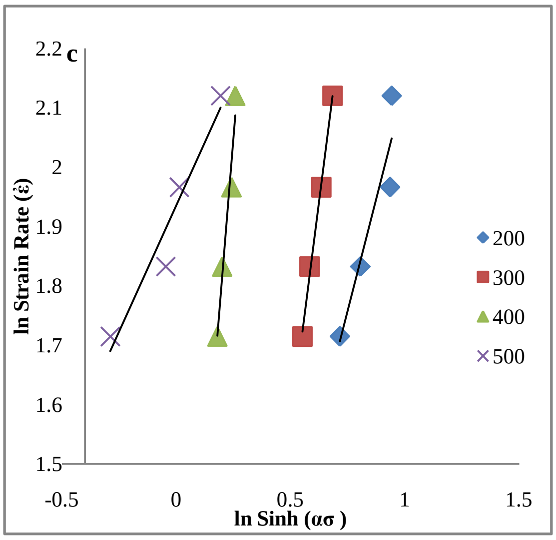

Fig.8. Relationship between ln strain rate and ln [sinh (ασ)] for the powder compact RD=80% (a) RD=85% (b) RD=90% (c).

Fig.8. The value of ln $\dot{\varepsilon}$ and ln sinh (ασ) at constant temperature for different powder compacts with different relative densities. The average slope of the lines attained at a constant temperature for different compacts was used to calculate the value of n'

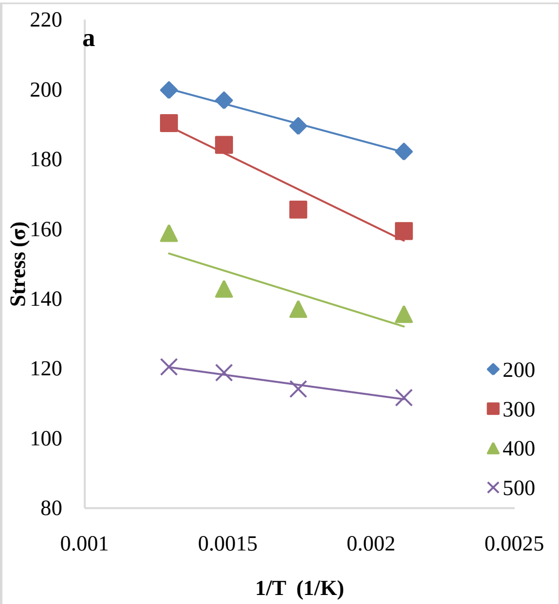

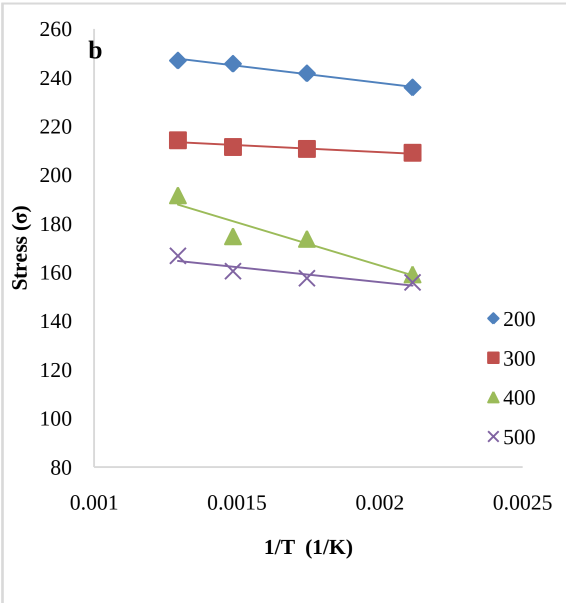

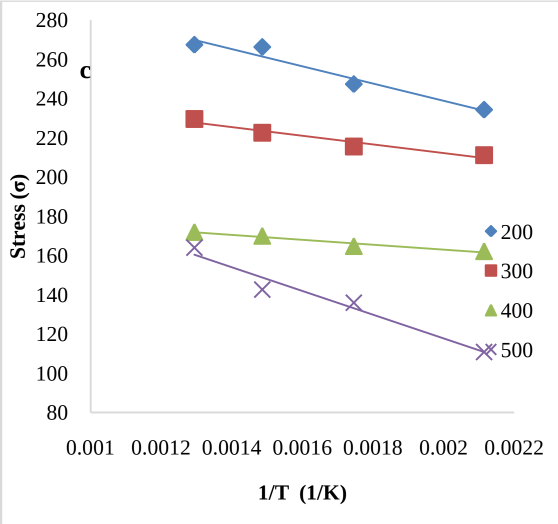

Fig.9. Relationship between stress and 1/T(K) for the powder compact with different relative densities (RD).RD=80% (a) RD=85% (b) RD=90% (c).

Fig. 9 can be fitted to second order polynomial curve (solid line), showing the evolution of beete, ln A, and Q with different relative densities, strain rate ,deformation temperature and flow stress of the powder compact can be expressed as follows (R2 is the multiple correlation coefficient of each adjustment)

$$Z= \dot{\varepsilon} \exp\left(\frac{Q}{RT}\right) = A\exp(\beta\sigma)$$

β =-0.2408(RD)^2+0.335(RD)-0.1045 ($R^2 = 1$)

ln (A)= 201.88 (RD)^2-313.1(RD)+128.78 ($R^2 = 1$)

Q= -765308(RD)^2+1E+06(RD)-601067 ($R^2 = 1$)

RD	β	ln A	Q
0.80	0.02865	7.5032	290864
0.85	0.02405	8.5033	304002
0.90	0.02285	10.5128	320966

e-ISSN 2320 –7876 www.ijfans.org
Vol.11, Iss.11, 2022
 UGC CARE Listed (Group -I) Journal

IPD	Temperature K	Strain rate $\dot{\varepsilon}$	Stress (σ) N/mm² Experimental	Stress (σ) N/mm² Calculated	Stress (σ) N/mm² Simulation	Load (L) KN Experimental	Load (L) KN Simulation
80%	473	0.12	182.179	189.3623	186	49.3	43.1
		0.14	189.482	193.7559	190	40.4	44.1
		0.16	196.817	194.7241	194	46.8	45
		0.18	199.815	201.6643	197	55.4	45.9
	573	0.12	159.3509	161.2216	154	41.6	38
		0.14	165.5328	165.8885	158	38.3	39.1
		0.16	184.0586	169.7069	162	43.2	40
		0.18	190.299	173.1011	165	46.7	40.8
	673	0.12	135.5815	136.614	154	35.4	32.2
		0.14	137.0702	140.432	158	38.7	33.1
		0.16	142.8239	144.250	162	42.3	34
		0.18	158.8691	147.645	165	46.4	34.8
	773	0.12	114.143	128.629	117	35	32.6
		0.14	111.6289	133.764	120	35.7	33.6
		0.16	120.4251	136.672	124	38.8	34.6
		0.18	118.8208	140.930	127	41.9	35.4
85	473	0.12	235.9063	262.754	242	72.3	70.2
		0.14	241.7719	281.095	258	76.9	75.1
		0.16	245.7312	298.312	274	81.1	79.7
		0.18	247.0646	313.658	288	83.3	83.8
	573	0.12	209.0879	225.325	207	68	60.2
		0.14	210.7013	241.42	222	69.2	64.5
		0.16	211.5598	256.391	236	70.3	68.5
		0.18	214.2228	269.866	248	76.4	72.1
	673	0.12	159.1622	195.917	180	50.7	52.4
		0.14	173.7873	209.979	193	57.3	56.1
		0.16	174.8395	223.453	205	63	59.7
		0.18	191.6823	235.056	216	70.3	62.8
	773	0.12	155.8637	176.667	163	49.6	47.2
		0.14	157.6465	187.862	174	58.3	50.3
		0.16	160.4957	201.152	185	64.5	53.8
		0.18	166.7933	211.995	195	67.5	56.7
90	473	0.12	234.2797	272.89	206	104.4	110
		0.14	247.3371	280.82	211	108.1	114
		0.16	266.4028	281.81	215	113.1	114
		0.18	267.5221	297.64	218	114.8	122
	573	0.12	211.1422	233.658	178	90.8	94.6
		0.14	215.5322	234.529	182	96.0	96.8
		0.16	222.6626	244.275	186	96.8	98.9
		0.18	229.5863	249.464	190	90.6	101
	673	0.12	162.2279	167.653	129	66.0	68.0
		0.14	164.8813	172.343	132	67.7	69.9
						68.2	

		0.16	170.0180	176.535	135	71.5	71.6
		0.18	172.0226	179.987	138		73.0
	773	0.12	146.1705	147.560	121	60.0	64.0
		0.14	154.9036	157.796	124	63.2	65.7
		0.16	158.4637	161.988	127	65.0	67.4
		0.18	159.5114	166.179	130	67.1	68.8

Conclusion:

The relationship between strain rate , deformation temperature, and flow stress of form compacts is described by the Zener-Hollomon parameter in an equation containing relative inexperienced density stipendiary deformation energy (Q) and material constant (β and A).

Depending on the relative inexperienced density, deformation energy of activation of the compacts ranged from 290864 to 320966 j/ mol that is sweet agreement with simulation values.

The relative inexperienced density contains a vital influence on the new deformation energy of activation and β constant of a compact. Because the relative inexperienced density will increase, giant hot deformation activation energies and lower β constant were ascertain.

The results of this study showed that the presence of pores within the structures of porous material reduces their resistance to deformation. Additionally the flow stress of powder compacts with high β constants is a smaller amount sensitive to deformation parameters like deformation temperature and strain rate.

The simulation and measured peak flow stresses of the powder compacts were in good agreement, , which confirms the applicability of the proposed modelling for the prediction of hot deformation flow stresses of case with different relative densities.

References

[1] R.E.D. Mann, R.L. Hexemer Jr., I.W. Donaldson, D.P. Bishop, Mater. Sci.Eng. A528 (2011) 5476–5483.

[2] B. Verlinden, L. Froyen, TALAT Lecture 1401: Aluminium Powder Metallurgy,European Aluminium Association, Brussels, Belgium, 1994.

[3] F. Bardi, M. Cabibbo, E. Evangelista, S. Spigarelli, M. Vukcevic ‘’An analysis of hot deformation of an Al-Cu-Mg alloy produced bypowder metallurgy’’

[4] J.C. Shao, B.L. Xiao, Q.Z. Wang, Z.Y. Ma∗, Y. Liu, K. Yang “Constitutive flow behavior and hot workability of powder metallurgy processed20 vol.%SiCP/2024Al composite”Materials Science and Engineering A 527 (2010) 7865–7872.

[5] R. Narayanasamy, V. Senthilkumar, K.S. Pandey "Some aspects on hot forging features of P/M sintered ironpreforms under various stress state conditions. Mechanism of materials 38 (2006) 367-386.

[6] S. Serajzadeh, A. Karimi Taheri, Mech. Res. Commun. 30 (2003) 87–93.

[7] H. Mirzadeh, A. Najafizadeh, Mater. Sci. Eng. A 527 (2010) 1160–1164.

[8] G. Chunlei, X. Yongdong, W. Mengjun, Mater. Sci. Eng. A 528 (2011) 4199–4203.

[9] N. Jin, H. Zhang, Y. Han, W. Wu, J. Chen, Mater. Charact. 60 (2009) 530–536.

[10] Y. Deng, Z. Yin, J. Huang, Mater. Sci. Eng. A 528 (2011) 1780–1786.

[11] H. Zhang, L. Li, D. Yuan, D. Peng, Mater. Charact. 58 (2007) 168–173.

[12] X. Huang, H. Zhang, Y. Han, W. Wu, J. Chen, Mater. Sci. Eng. A 527 (2010)485–490.

[13] M. Rajamuthamilselvan, S. Ramanathan, J. Alloys Compd. 509 (2011) 948–952.

[14] G. Chunlei, X. Yongdong, W. Mengjun, Mater. Sci. Eng. A 528 (2011) 4199–4203.

[15] M.R. Rokni, A. Zarei-Hanzaki, A.A. Roostaei, A. Abolhasani, Mater. Des. 32 (2011)4955–4960.

[16] W. Li, H. Li, Z. Wang, Z. Zheng, Mater. Sci. Eng. A 528 (2011) 4098–4103.

[17] M. yan Zhan, Z. Chen, H. Zhang, W. Xia, Mech. Res. Commun. 33 (2006) 508–514.

[18] P.T. Wang, M.E. Karabin, Powder Technol. 78 (1994) 67–76.

[19] P.T. Wang, Powder Technol. 66 (1991) 21–32.

[20] P.T. Wang, M.A. Zaidi, Powder Technol. 66 (1991) 9–19.

[21] S. Serajzadeh, A. Karimi Taheri, Mech. Res. Commun. 30 (2003) 87–93.

[22] H. Mirzadeh, A. Najafizadeh, Mater. Sci. Eng. A 527 (2010) 1160–1164.

[23] R.E.D. Mann, R.L. Hexemer Jr., I.W. Donaldson, D.P. Bishop, Mater. Sci. Eng. A528 (2011) 5476–5483.

[24] G.Y. Lin, Z.F. Zhang, H. Zhang, D.S. Peng, J. Zhou, Acta Metall. Sinica (EnglishLetters) 21 (2008) 109–115.

[25] H. Li, Z. Li, M. Song, X. Liang, F. Guo, Mater. Des. 31 (2010) 2171–2176.

[26] C. Zener, J.H. Hollomon, J. Appl. Phys. 15 (1944) 22–32.